Current Research in Food Science 8 (2024) 100688

Contents lists available at ScienceDirect

Current Research in Food Science

journal homepage: www.sciencedirect.com/journal/current-research-in-food-science

Pleurotus ostreatus is a promising candidate of an edible 3D printing ink: Investigation of printability and characterization

Rui Liu [a], Qiuhui Hu [a], Gaoxing Ma [a], Fei Pei [a], Liyan Zhao [b], Ning Ma [a], Fan Yang [a], Xiao Liu [b], Anxiang Su [a,*]

[a] College of Food Science and Engineering, Nanjing University of Finance and Economics/Collaborative Innovation Center for Modern Grain Circulation and Safety, Nanjing, 210023, China
[b] College of Food Science and Technology, Nanjing Agricultural University, Nanjing, 210095, China

ARTICLE INFO

Handling editor: A.G. Marangoni

Keywords:
3D printing
Pleurotus ostreatus
Stability
Molecular interaction
Rheological properties

ABSTRACT

The 3D printing (3DP) technology shows great potential in the food industry, but the development of edible ink is currently insufficient. *Pleurotus ostreatus* (*P. ostreatus*) emerges as a novel promising candidate. In this study, a mixed ink was obtained by incorporating butter into *P. ostreatus*. The effects of different ratios of *P. ostreatus* and butter, as well as the influence of ink steaming were investigated on 3D printed products. The results indicated that all inks of the *P. ostreatus* system exhibited positive shear-thinning behavior, and the system maintained stable intermolecular hydrogen bonding when *P. ostreatus* powder concentration was 40 % (w/v). Furthermore, the L* value of the system was elevated for butter adding. The system with steaming exhibited superior stabilized molecular structure compared to the native system, particularly with a steaming duration of 5 min, showcasing its outstanding supporting capacity. This study suggests that *P. ostreatus* is a promising candidate in 3DP for the development of an edible ink that promotes innovation and nutritional food.

1. Introduction

As a promptly progressive additive manufacturing method, 3D printing (3DP) technology has been utilized in the food industry (Guo, et al., 2019). Compared with traditional food production methods, 3DP technology offers enormous advantages, such as the elimination of manual operation or mold making, the ability to match ingredients according to nutritional needs, and the customization of complex structures based on individual preferences (He, et al., 2023). However, for the recognition and further development of 3DP in the food industry, it is essential to develop more edible inks with excellent nutritional and printing performance (Qiu, et al., 2023). The previous 3DP ink mainly included potatoes and other raw materials with high starch content, thickener-assisted raw materials with high water content (Shi, et al., 2022), and innovative resources like insects, cell-cultured plant flesh and other novel raw materials (Baiano, 2022; Ji et al., 2022a, b). But most studies only focused on the edibility and printability, being short of the nutritional value and individual preferences. For example, the inks designed for children need vibrant colors and appealing appearances, while those for the elderly should be sweetly swallowed (Jiang, et al., 2022), all while ensuring the nutrition of food. The development of edible ink still faces challenges in meeting printing performance and consumer requirements for nutrition, flavor, and texture (Guénard-Lampron, et al., 2021; Fernandes et al., 2023). Therefore, *Pleurotus ostreatus* (*P. ostreatus*) was selected as a novel and promising edible ink with high nutritional vaue in this study.

The protein, polysaccharides and terpenes, and abundant essential amino acids in edible fungi supply exceptional nutritional value and biological activity, making them excellent food raw materials (Ji et al., 2023). Furthermore, the protein rich in *P. ostreatus* brings it a unique taste, positioning it as a prospective low-calorie vegan protein source (Hamza, et al., 2023). Moreover, studies have confirmed that the protein and polysaccharides in *P. ostreatus* contribute to stable rheological properties and functional activity (Wang, et al., 2021). The study has found hopeful effect of the protein in *P. ostreatus* on enhancing the viscosity of printing ink (Liu, et al., 2022a, b). This indicates that *P. ostreatus* has the potential to become a new ink that combines nutritional quality and printing performance. Notably, the dietary fiber in *P. ostreatus* may affect the extrusion and molding of ink (Liu, et al., 2022a, b), so it is also necessary to investigate the practicality and

* Corresponding author.
E-mail address: xiangansu@nufe.edu.cn (A. Su).

https://doi.org/10.1016/j.crfs.2024.100688
Received 21 November 2023; Received in revised form 6 January 2024; Accepted 25 January 2024
Available online 1 February 2024

printing performance of *P. ostreatus* ink. The nutritional components in *P. ostreatus* detected in our previous research confirmed great potential for its utilization (Xu, et al., 2022a, b). In this study, *P. ostreatus* was used as a novel 3DP ink for building a stable system primarily relying on the hydrogen bonding forces formed between macromolecules. Then butter and steaming were added to improve the sensory quality and printing stability. The printable performance and structural stability were assessed through the rheological properties and molecular structure analysis. The influence of protein, polysaccharides, and lipid in the ink on the system was also examined. This study holds promise in providing an approach for precise manufacturing in edible fungi full valuable products and serves as a reference for enhancing the quality of 3DP food.

2. Materials and methods

2.1. Materials

The dried *P. ostreatus* was provided by Henan Mushroom Taro Food Co., Ltd., and butter was purchased from the local Suguo supermarket (Nanjing, China). All other chemicals were reagent grade.

The percentage in the ink name is calculated based on the ratio of the component to the volume of water. The Butter-0 % present in the experiment and data is equivalent to POP-40 %, as a control for adding different amounts of butter; Steaming-0min is the same as Butter-4 % as a control for different steaming times. POP: *P. ostreatus* powder.

2.2. Ink preparation method

The mixed ink with *P. ostreatus* as the main material was prepared in this work. Based on the preliminary experiment, the preparation results under all conditions were listed in Table 1. After grinding and sieving under 100-mesh, 15 g, 17.5 g, 20 g, 22.5 g and 25 g of *P. ostreatus* powder (POP) were weighed separately into 50 mL of ultra-pure water and stirred (MR Hei Tec, Heidolph Instruments, Schwabach, Germany) for 200 rpm under the action of magnetic force. The inks of POP with concentrations of 30 %, 35 %, 40 %, 45 % and 50 % (w/v) were prepared. The mixed ink of POP and butter was prepared in the equivalent way. The amount of butter was calculated by water. The steamed ink was obtained from the former experimental treatment. Then the mixed ink was placed in a 100 mL beaker. And the beaker was sealed with cling film and heated in the steamer (Midea, MZ-SYH26-2CB, Foshan, China) for 5, 10, and 15 min after the temperature of the steamer reached 100 °C. When the ink was cooled to 25 °C, the subsequent experiments could be performed.

2.3. Rheological analyses

A rheometer (MCR302, Anton Par, Graz, Austria) was applied to determine the rheological properties of ink gels at 25 °C. The diameter of the parallel plate was 50 mm and the gap was 1000 μm. All inks were equilibrated to stand for 3 min at 25 °C before starting the test to ensure the stability of the experiment. The shear rate was first set to 0.01–100 s^{-1} for the static rheological test, and the apparent viscosity was recorded to produce a static rheological profile. For determining the linear viscoelastic zone of ink, strain scanning experiments were conducted at 1 Hz with a strain range of 0.01 %–100 %. Then dynamic rheological tests were conducted with a constant of 0.1 % strain (in the linear viscoelastic region) within the range of 1–100 Hz. The values of energy storage modulus (G'), loss modulus (G") and tan δ (tan δ = G"/G') were obtained to produce dynamic rheological characteristic curves. All tests were repeated three times at 25 °C, and the average values were used for data analysis.

Table
1The formulation of different inks in printing gel system.

Ink	POP (g)	Butter (g)	Water (mL)	Steaming (min)
POP-30 %	15	0	50	0
POP-35 %	17.5	0	50	0
POP-40 %	20	0	50	0
POP-45 %	22.5	0	50	0
POP-50 %	25	0	50	0
Butter-0 %	20	0	50	0
Butter-4 %	18	2	50	0
Butter-8 %	16	4	50	0
Butter-12 %	14	6	50	0
Steaming-0min	18	2	50	0
Steaming-5min	18	2	50	5
Steaming-10min	18	2	50	10
Steaming-15min	18	2	50	15

2.4. Printing process

The FOODBOT-MF 3D food printer (FoodBot-D1, Shin-nove, Hangzhou, China) was utilized. The final parameter settings for 3DP were based on preliminary experimental optimization: the filling rate was 100 %, the nozzle diameter was 1.2 mm, the nozzle moving speed was 30 mm/s, the nozzle height was 1.2 mm, and the printing layer height was 1.2 mm. At room temperature of 25 °C, the printability of all inks was estimated utilizing a solid cylinder with a diameter of 20 mm and a height of 15 mm designed by Rhinoceros 7.0. And each ink was repeatedly printed three times. This investigation also printed flower, small yellow duck and other attractive structures.

2.5. Printing accuracy and formability index evaluation

The bottom diameter accuracy (the ratio of the length of the set model to the length of the actual printed sample) and the height accuracy (the ratio of the height of the set model to the height of the actual printed sample) were used as two precise indicators to evaluate the printing accuracy of test systems. The printing accuracy was reflected by calculating the height accuracy difference and diameter accuracy difference between the printed sample and the model in this experiment. The supporting performance of all printing systems was evaluated by the height of the printed cylinder, and the printing formability was evaluated by the printing accuracy. Each group of experimental data was repeatedly measured five times.

2.6. Color measurement

In this study, 3DP ink was obtained from different ingredients and processing methods, which had a great impact on the color and retention of printing samples. Therefore, the CIELab color parameters (including L*, a*and b*) of the printing system at the initial and 0.5 h were measured. A calibrated colorimeter (MC-5, Konica Minolta Co., Osaka, Japan) was used to perform color measurements. Then, a layer of transparent cling film was spread on the sample to avoid the lens being smudged. The color was expressed by L* (lightness), a* (redness/greenness) and b* (yellowness/blueness), and the larger the L* was, the brighter the sample held.

2.7. Microstructure analysis

The microstructure was observed and recorded by using scanning electron microscopy (SEM). First, the printed samples were uniformly sliced, dried in a vacuum freeze dryer for 54 h, and then subjected to vacuum ion sputtering for gold plating. Thereafter, the microstructure was observed under SEM magnification of 200 times. The acceleration voltage of the SEM was set to 15 kV.

2.8. Fourier transform infrared (FT-IR) spectroscopy

An IR200 infrared spectrometer (Nicolet IR200, Thermo Scientific, Madison, WI, USA) was operated to obtain the FT-IR spectra of the

lyophilized samples. Each sample was sieved and ground in an agate mortar with spectrally pure potassium bromide (KBr, spectroscopic grade) at weight ratio of 1:100. The mixed powder was pressed into thin slice and detected on the machine with air as background, wavelength range 4000–500 cm^{-1} and 32 scans to obtain the transmittance curve.

2.9. Moisture distribution state determination

An NMI20 analyzer (Niumag, Suzhou, China) was applied for the determination of the moisture distribution status. Before testing, the sample was calibrated with oil sample in Free-Induction-Decay (FID) mode, then measured by the CPMG sequence. The magnetic field strength was 0.5 T and the magnetic field temperature was 32 °C for the test. The sample was weighed 3 g in a glass injection vial and measured in a Ø30 mm × 200 mm glass tube with the following parameters: TW (ms) = 2000, NECH = 2500, spectrum width (SW) = 100 kHz, and the number of iterative scans (NS) = 4. Inversion analysis was obtained with the number of iterations set to 10,000.

2.10. Statistical analysis

The data of the experiment were analyzed using SPSS analysis software and charted by Origin 9.0. A single factor analysis of variance (ANOVA) and Duncan test (DMRT) were used to perform multiple comparisons at the 0.05 significance level. The significant differences were indicated by different letters ($P < 0.05$).

3. Results and discussion

3.1. Hypothesis model

The effect of *P. ostreatus* mixed edible ink on 3DP was investigated in this part, aiming to establish a stable 3DP system for *P. ostreatus*. And a hypothesis of structure-activity relationship is proposed (Fig. 1). The interaction between proteins and polysaccharides in *P. ostreatus* and their water holding properties will mainly rely on hydrogen bonding forces, resulting in a dense structure of the printed gel. The macromolecular substances in *P. ostreatus* exhibited good viscosity and structural stability, but the lipid in butter may influence the combination with water. However, the protein denaturation and carbohydrate aging after cooling will help the mixed ink tend to stabilize in ink steaming treatment. In this situation, the hydrogen bonds in the ink system are stable and orderly. And the ink will change from weak gel to strong gel with more orderly and stable arrangement of molecular. These hypotheses will be systematically verified and discussed through subsequent rheological performance, molecular structure, and other tests.

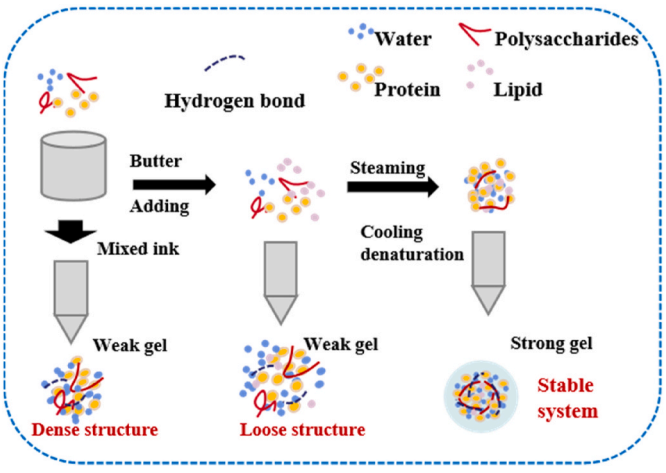

Fig. 1Hypothesis model: Interactions between multiple macromolecules in the printing system of *P. ostreatus* mixed ink.

3.2. Rheological properties

3.2.1. Static rheological analysis

Static rheology testing is utilized to reflect the change of shear stress and viscosity with shear rate when the structure of the printing system is broken (Adedeji, et al., 2022; Wedamulla et al., 2023). Fig. 2A presented the measurement of static rheology of 3DP system with different amounts of POP. The apparent viscosity of the ink increased from 65, 500 Pa s to 17,400 Pa s at the shear rate of 0.01 s^{-1}. The potential reason for this is that the hydrogen bond content in the hydrocolloid increases with the expanding of POP content, prompting the stabilization of the system structure (DuZhou et al., 2022). Interestingly, the apparent viscosity of the inks decreased with the multiplication of butter (Fig. 2B). The possible reasons are as follows. First, a related study has shown that water molecules can be dispersed by the oil molecule (Abdel-Aal, et al., 2020), and the addition of butter may inhibit the dissolution of POP in water. Moreover, the reduction of POP content reduces the content of the protein (Liu, et al., 2022a, b) that can form stable structure. As the previous study reported (Chen, et al., 2023), ternary complexes can not be formed in a system model composed of rice starch, rice protein, and lipids. Secondly, free fatty acids with strong steric hindrance and electrostatic repulsion may delay the swelling of starch particles and further inhibit their interaction with water molecules. Fig. 2C displayed that the apparent viscosity of the ink effectively increased with steaming treatment compared to untreated ink. It may be attributed to the steaming enhancing bonding between thermally denatured protein components and polysaccharides, thereby increasing the internal organizational strength of the ink (Lv, et al., 2023).

Previous studies have reported that the interaction between polysaccharides and proteins in *P. ostreatus* also makes a difference to the adhesiveness and cohesiveness (Sołowiej, et al., 2023). The rheological properties of protein-rich gel can be enhanced by the concentration increasing of small-molecular-weight saccharides. In addition, the change in shear modulus caused by the addition of xylose may help strengthen protein-saccharide, protein-water, and/or protein-protein interactions (Wen, et al., 2022). It can be inferred that the proteins and polysaccharides in *P. ostreatus* contribute to the stability for the viscosity and structure of the ink system, besides providing nutrition. Herein, the viscosity of all gels decreased with the increase of the shear rate, which was referred to shear thinning property of non-Newtonian fluids. This phenomenon as a rheological performance indicator is beneficial for human chewing and swallowing, demonstrating the 3DP suitability of *P. ostreatus* ink (He, et al., 2021).

3.2.2. Dynamic rheological analysis

The storage modulus (G') and loss modulus (G") represent the ability of the system to resist elastic deformation and the amount of energy lost during viscous deformation, respectively. The ratio of G" to G' is defined as the loss angle tangent (tan δ) (Wedamulla, et al., 2023). From Fig. 2D, the G' of 3DP inks was positively correlated with the amount of POP, suggesting that *P. ostreatus* brought excellent resistance to deformation for the printing system. G" is often used to characterize the viscosity of the gel. A larger G" is conducive to the formation of a dense and homogeneous gel structure, thus effectively fixing the components (Jiang, et al., 2019).

The oil molecules may interfere with the original molecular arrangement of *P. ostreatus* (Fernandes, et al., 2023), so that the addition of butter does not ideally enhance the G" of the inks (Fig. 2E). However, it was shown that G" was effectively improved with the multiplication of steaming time, indicating that steaming was conducive to enhancing the stability of the internal molecular structure of printing system. This was consistent with the later research results. Lin et al. (2024) reported that after thermal induction, the G′ and G″ of the cooled ink increased, indicating that the network structure of gel strengthened formed by

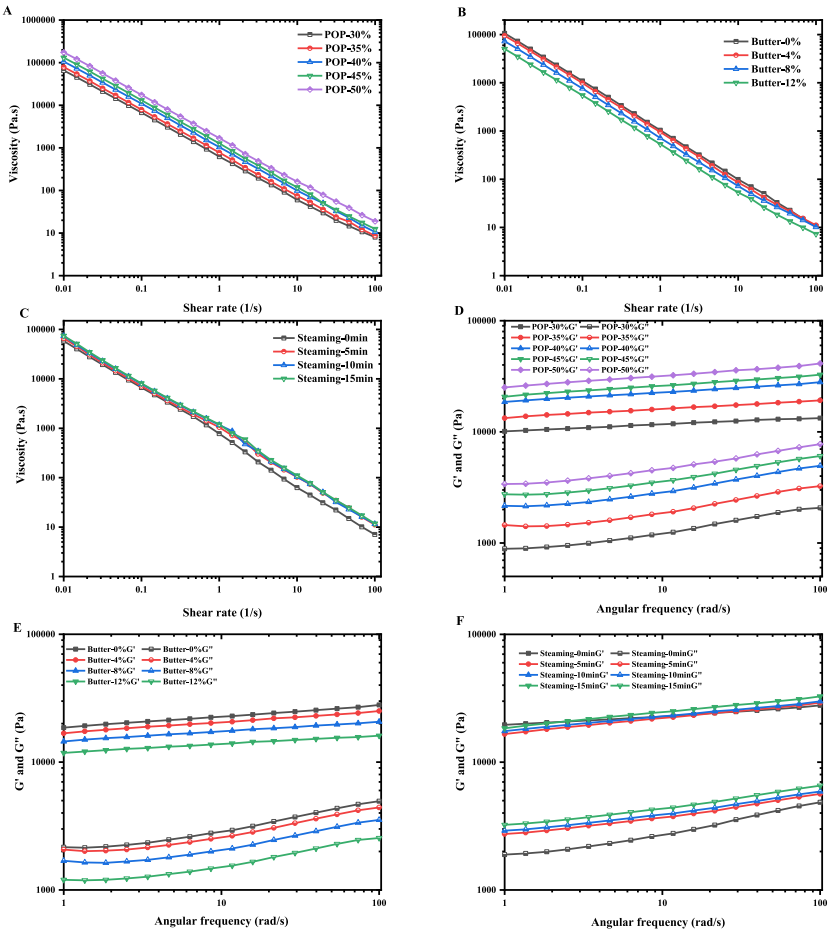

Fig. 2Changes of the rheological properties of different ink gels. The viscosity of different inks (A–C), storage modulus (G') and loss modulus (G") of different inks (D–F). The Butter-0 % present in the experiment and data is equivalent to POP-40 %, as a control for adding different amounts of butter; Steaming-0min is the same as Butter-4 % as a control for different steaming times. POP: *P. ostreatus* powder.

protein molecules through hydrogen bond interactions. Moreover, it can be found that all tan δ was less than 1. When the value exceeds 1, the system represents the viscous behavior of a partially liquid form, whereas a value less than 1 indicates the elastic behavior of a partially solid form (Zhang, et al., 2023). Therefore, it indicated that the solid form can still be provided including butter addition. As a popular food with nutrition and flavor, butter can be used to regulate the rheological properties of the system that is difficult to extrude with high viscosity in future research.

3.3. Printing effect analysis

Accuracy indicators can intuitively represent the degree of fit between 3DP samples and models, thereby assessing the printing support ability of the system. The accuracy deviation of sample diameter with different amounts of POP indicated all sample diameters surpassed the model setting (Fig. 3A). This may be resulted by the water absorption expansion of the gel and the extrusion line width being larger than the model setting (Zhang, et al., 2023). As displayed in Fig. 3a, sample collapse caused by the ink gel with too low concentration can also affect the printing diameter, involving the self-supporting ability. Comprehensively, the printing system with POP-40 % retains a smooth, complete surface and clear lines, catching preferable formability and suitability for further research. Besides, the height accuracy for *P. ostreatus* system mixed with butter ranged from 99.87 % to 131.82 %, reflecting the gradual loss of support performance for the system. The possible reason is the sample collapse resulted by thinning and strong fluidity of the ink as changes in molecular structure (He, et al., 2023). Therefore, the ink was steamed to improve structural stability. It showed that the diameter accuracy difference of the ink steamed for 5 min after 3DP decreased. And the integrity and filling effect of Steaming-5min stayed ahead of other times (Fig. 3l and n). Nevertheless, the accuracy of the Steaming-10min and Steaming-15min gradually deteriorated. This may be due to structural changes in proteins under steaming conditions and the evaporation of water in the ink, resulting in structural voids (Fan, et al., 2022). Based on the rheological analysis results and similar observations reported previously, it is anticipated that the viscosity of *P. ostreatus* hybrid ink was enhanced by means of steaming, thereby maintaining the printing performance of the ink (Lv, et al., 2023).

3.4. Color change analysis

Color is a prominent factor determining the acceptance of 3DP products by consumers. But the color of edible fungi tends to undergo oxidative browning during processing and storage. Compared with the initial stage of printing, the L* value of all samples decreased after 0.5 h (Fig. 4). This may be attributed to the universal occurrence of oxidation browning in *P. ostreatus* when combined with water in the air (Hsieh, et al., 2020). As the samples are exposed to the air, moisture is removed, leading to a weakening of scattering intensity on the inner and outer surfaces as moisture content decreases (DuZhou et al., 2022). And the

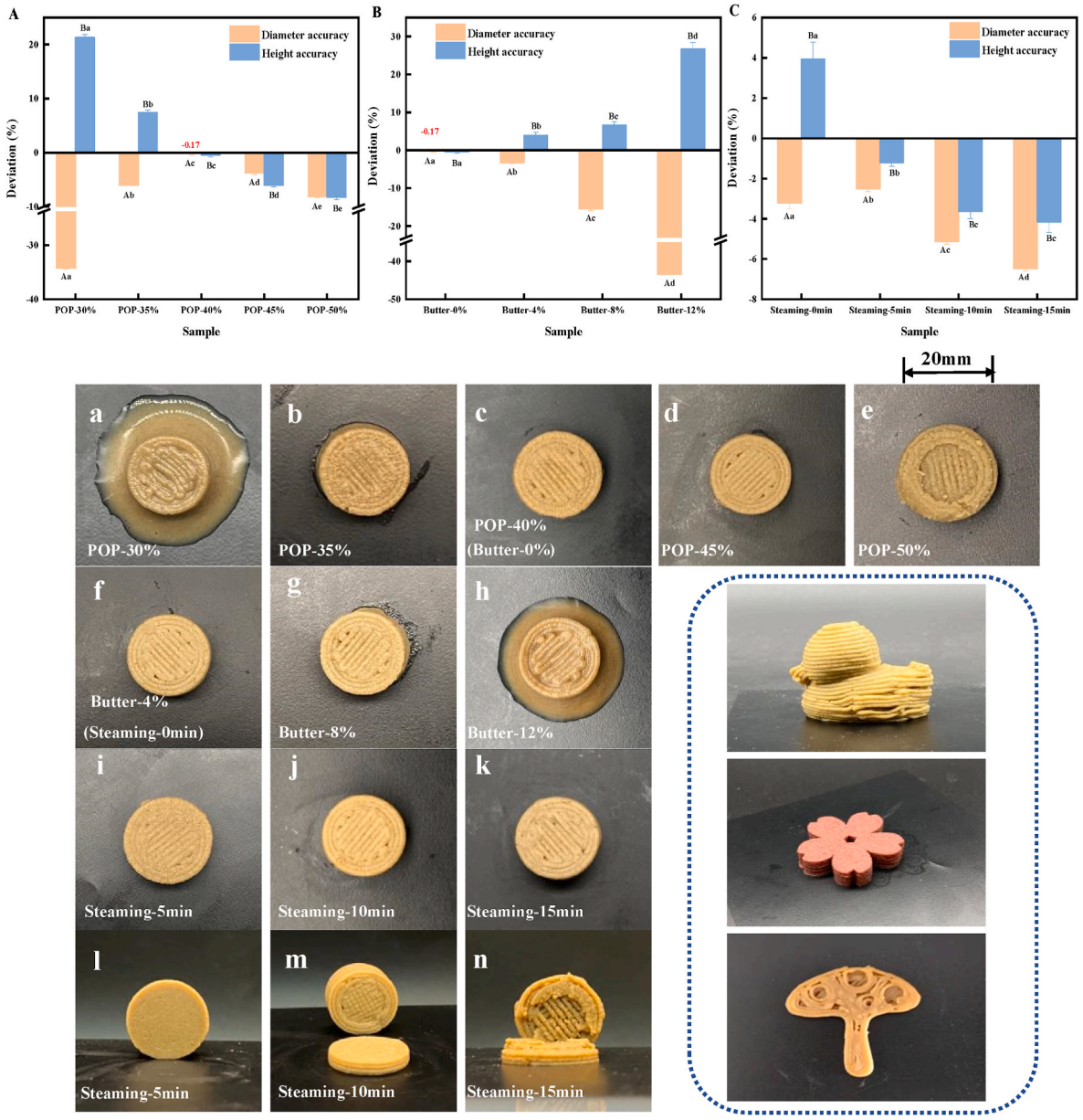

Fig. 3The deviation in printing diameter accuracy and height accuracy of different printing gel samples (A–C). Error bars represent standard deviations of the mean. A and B on the column chart represent different measurement standards. Mean values not sharing the same lowercase letters are significantly different from each other ($P < 0.05$). The appearance of different printing gel samples: POP-30 % (a), POP-35 % (b), POP-40 % (c), POP-45 % (d), POP-50 % (e), Butter-4 % (f), Butter-8 % (g), Butter-12 % (h), Steaming-5min (i, l), Steaming-10min (j, m), Steaming-15min (k, n). The situation of the printing samples corresponding to the steaming time detached from the printing platform (l, m, n). POP: *P. ostreatus* powder.

reaction between the internal protein and carbohydrate can also cause color change (Nooshkam, et al., 2019).

In this research, butter was added to the *P. ostreatus* ink to observe the sensory effect of the printing system. It was something of a satisfaction to find that the L* value of the samples mixed with butter increased. And the b* value was also enhanced with the addition of more butter. The incorporation of fat in butter limits the contact between enzymes and substrates in Enzyme catalysis for *P. ostreatus* (Zheng, et al., 2023). The addition of butter separated the connection between the ingredients in the ink. And the brightness, yellowness and whiteness of butter are higher than that of *P. ostreatus*, which can bring better appearance to 3DP products (Méndez-Cid, et al., 2017). It was worth noting that the change rate of L* value of the printing system by the steaming ink after 0.5 h was slightly reduced, except for the increase of L* value. The existing study has shown that the moisture in the steaming ink partially evaporates and takes away some impurity pigments in the system (Guo, et al., 2021). On the other hand, according to the infrared analysis, the molecular structure of the steaming ink is more stable, so the composition in the system can be changed without simplicity. It shows that the addition of butter can effectively improve the whiteness and brightness of the printing system, and steaming can maintain brightness, significantly enhancing the sensory quality of the *P. ostreatus* printing system.

3.5. Microstructure

The microstructure of all printed samples was shown in Fig. 5. Compared with POP-30 %, the internal layers of POP-35 % and POP-40 % were dense and orderly with the relatively large surface area. In POP-50 % sample, the gap between the layers became large. It may be

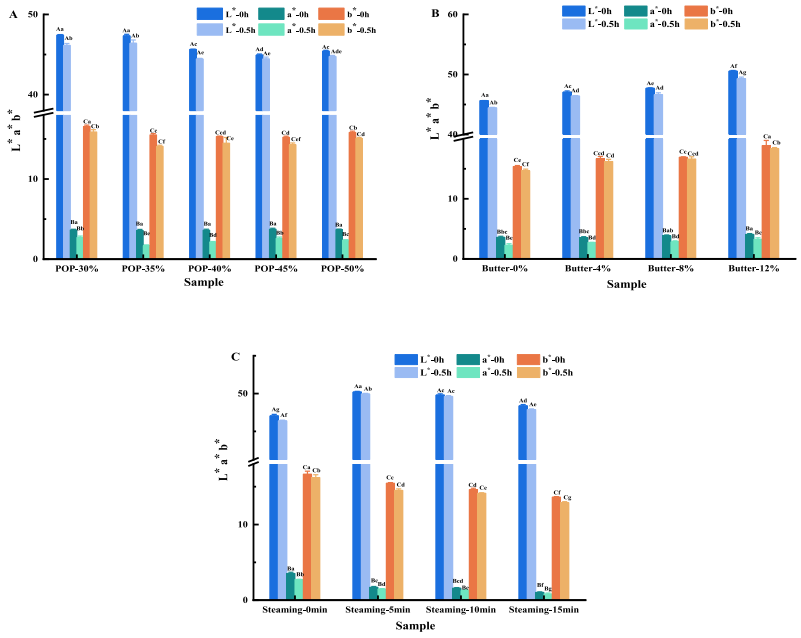

Fig. 4The L*, a*and b* values of different printing gel samples (A–C). Error bars represent standard deviations of the mean. A, B and C on the column chart represent different measurement standards. Mean values not sharing the same lowercase letters are significantly different from each other ($P < 0.05$). POP: *P. ostreatus* powder.

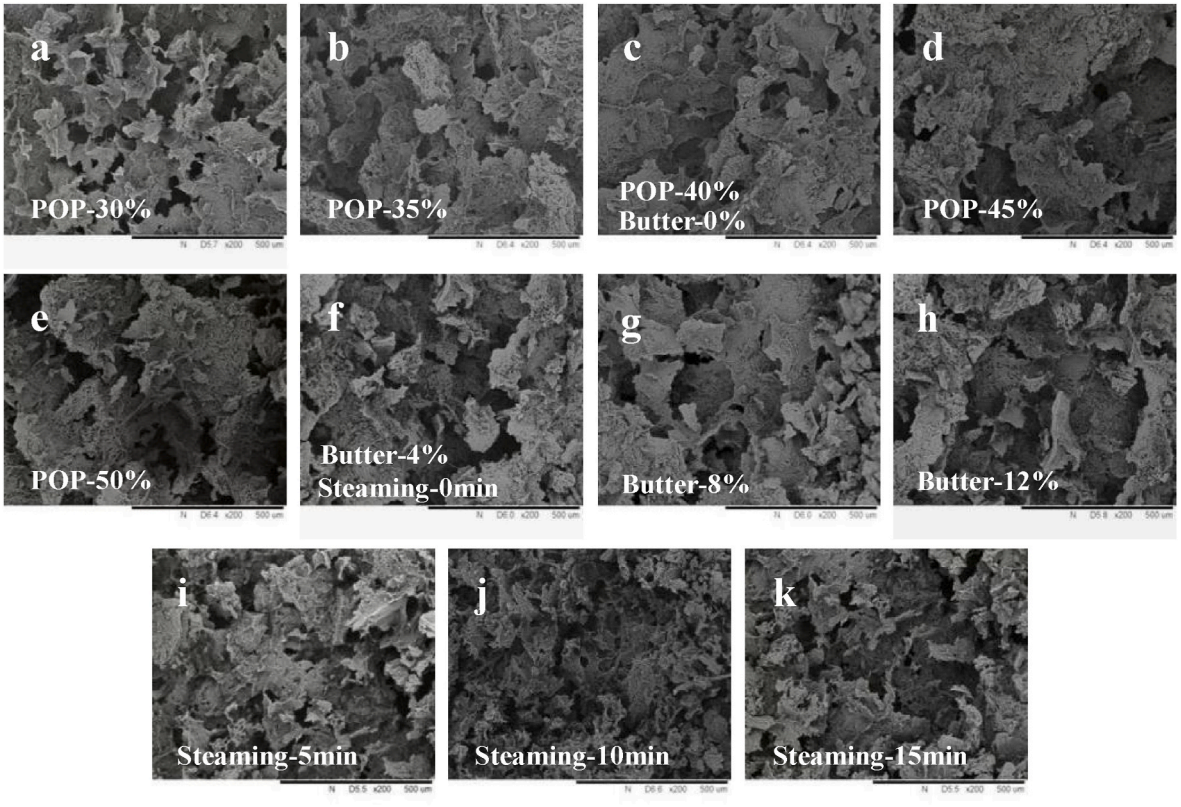

Fig. 5Microstructure behavior of different printing gel samples: POP-30 % (a), POP-35 % (b), POP-40 % (c), POP-45 % (d), POP-50 % (e), Butter-4 % (f), Butter-8 % (g), Butter-12 % (h), Steaming-5min (i), Steaming-10min (j), Steaming-15min (k). POP: *P. ostreatus* powder.

because insufficient hydration at the initial stage of the formation of the ink makes to the forming of the large spatial organization structure between macromolecular substances such as polysaccharides in *P. ostreatus* (Liu et al,.2023). It indicated that the mutual bonding effect between the printing and deposition layers was better in the system of POP-40 %. But the surface area of the lamellae inside the sample became smaller, and fragments and fractures gradually appeared with the increase of the butter content (Fig. 5f-h). This may be caused by the

expansion and physical retention of carbohydrate in the butter matrix reducing the water holding capacity of the sample and affecting its internal support capacity (Anukiruthika, et al., 2020). Additionally, the fat molecules in butter interfere with the interaction of polysaccharides and proteins in *P. ostreatus* and delay the formation of ordered structure, leading to changes in the structure and texture of the printing system (Zhao, et al., 2023). This will lead to a decrease of the laminated bonding ability in gels, holding consistent with the apparent viscosity decline of the ink. Relatively dense and uniform pores were obviously observed in the printed samples after steaming treatment, and the interlayer was more compact. This is likely due to the improvement of the order of molecules in gel by steaming treatment. Moreover, the protein denaturation through thermal steaming maintains ordered structure that is not easily affected by printing (Xu, et al., 2022a, b). The printing system of steamed ink has a smaller pore size, which is mainly due to the denser and more compact network of protein molecules of *Pleurotus ostreatus*, resulting in smaller cavities (Wen, et al., 2022). In addition, Guerrero et al. (2012) found that based on the crosslinking reaction, the more compact structures during heating occurred by adding small molecular weight saccharides to protein. What's more, the proteins and polysaccharides in *Pleurotus ostreatus* may also form a more compact structure. However, the microstructure of steaming-15min became rough and uneven. Excessive steaming time may cause the volatilization of water in the ink, leading to internal drying and cracking (Lv, et al., 2024). The research (Ma, et al., 2024) found that the migration in the direction of heat transfer of lipids caused by heating could lead to a more ordered and stable protein structure. However, heating for a period of time can promote protein aggregation, but excessive heating can damage protein aggregates (Wang, et al., 2020). From the microscopic results, steaming ink is conducive to improving the stability of the internal structure of the *P. ostreatus* system.

3.6. Molecular structure analysis

Infrared spectroscopy is utilized to analyze the intermolecular structure and interaction force to study the hydrogen bond strength. According to Fig. 6A, the absorption peak near 2900 cm^{-1} generally refers to the presence of the C–H bond and the wave number of bond energy decreased as the interaction between substances increased in intensity (Thongcharoenpipat, et al., 2023). The C–H bond absorption peaks of POP-35 % and POP-40 % appeared at 2926 cm^{-1}, which was slightly shifted to the lower wave number compared with other groups. This declares that when an appropriate amount of POP is dissolved in water, the hydrogen bonds with superior stability will be generated by the interaction between macromolecules and water (Yu, et al., 2022). In addition, the absorption peak at 2855 cm^{-1} may be formed by C–H asymmetric stretching vibration in fat. 1745 cm^{-1} is related to carbohydrate lipid complex (Barragan-Martinez, et al., 2022). This absorption peak intensity is enhanced with the growth of butter amount. It indicates that the carbohydrate in the system is combined with a certain amount of lipid, which is also one of the reasons for the changing structure stability of the printing system. At the same time, it can be found that the absorption peak intensity of about 3400 cm^{-1} commonly used to describe the content of the O–H bond decreased with the increase of butter content (Fig. 6B). This may be that the increase of fat content in the gel led to the weakening of the interaction between polysaccharides and water (Wen, et al., 2021). However, with the increase of steaming time, the peak gradually shifted to a lower wave number, and the height gradually increased. This shift is likely due to the tensile vibration of –OH, which promotes the increase of intermolecular hydrogen bond content and structural stability (Zheng, et al., 2020).

3.7. Water distribution state analysis

The content, distribution, fluidity and change of water are important factors that affect the stability of the food. As shown in Fig. 7A, there were three signal peaks representing bound water (T_{21}), fixed water (T_{22}) and free water (T_{23}) (Kong, et al., 2023). T_{21} appeared when the relaxation time was less than 10 ms, indicating water with poor fluidity in the system. The water relaxation time was closer to 0 ms as the content of POP increased. According to earlier studies, the fluidity of water molecules largely depends on the network structure of materials. In addition, the macromolecular polymers such as polysaccharides and proteins in the system are tightly bound to water, the structure of the

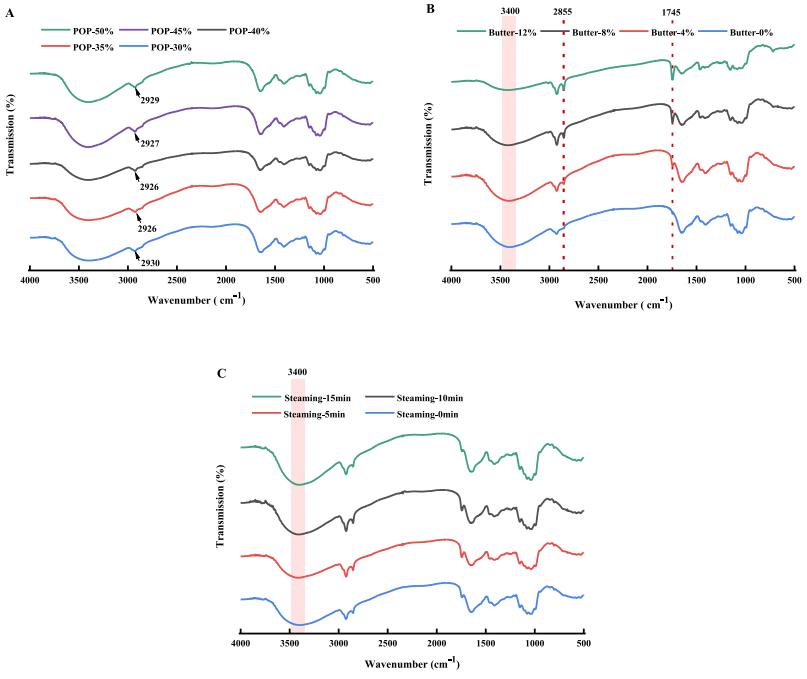

Fig. 6Fourier transform infrared (FT-IR) absorption behavior of different printing gel samples (A–C). POP: *P. ostreatus* powder.

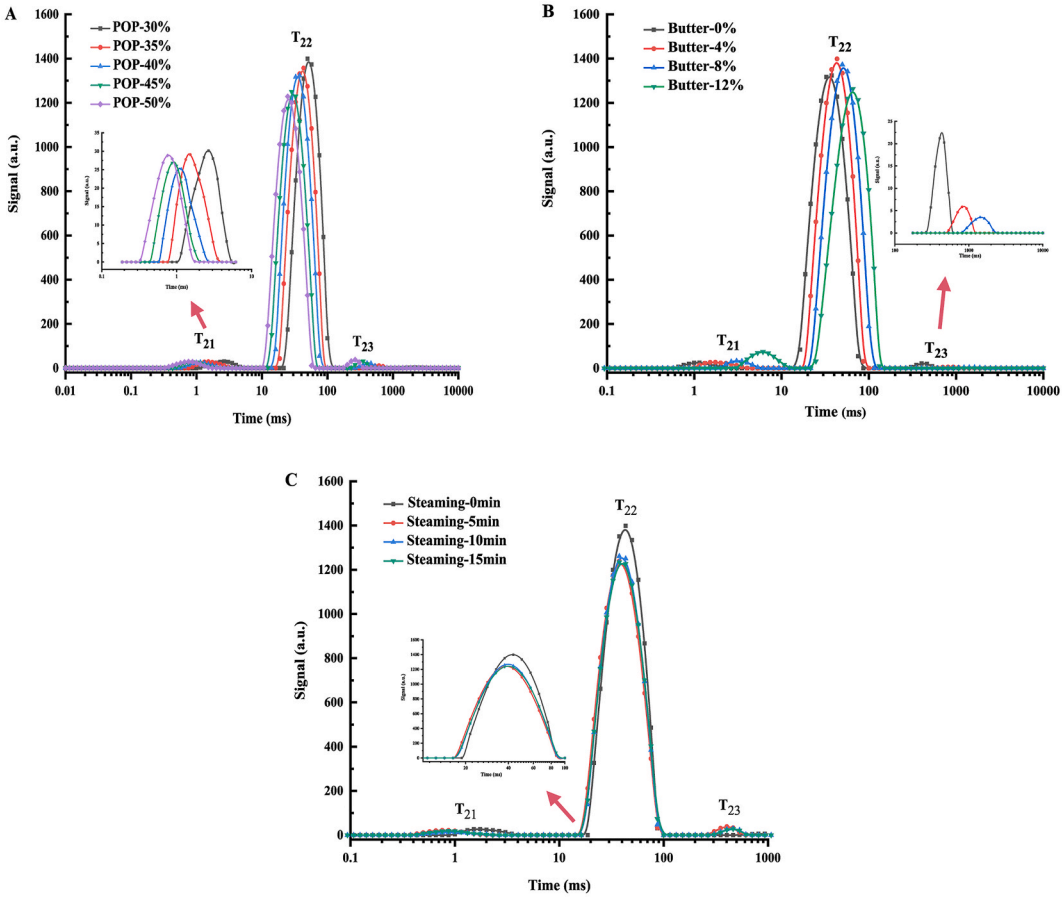

Fig. 7Moisture distribution of different printing gel samples (A–C). POP: *P. ostreatus* powder.

system tends to stabilize and the fluidity of water is not ideal (Nie, et al., 2022). This indicates that the higher POP content leads to a more stable internal structure in the printing hydrogel system. The large lateral relaxation time (T_{22}) reflects the high degree of freedom and fluidity of water molecules, which means that the material is extruded more smoothly from the nozzle. However, combined with POP-30 % printing accuracy result, excessive fluidity of water within the gel led to molding difficulties. Based on our previous research, the ability of extrusion and morphology maintenance demonstrate excellent when the amount of POP is about 40 % in the printing system.

As shown in Fig. 7B, with the increase of the amount of butter, the relaxation time of the signal peak in the low-field nuclear magnetic resonance spectrum became longer, indicating that the addition of butter enhanced the fluidity of water molecules in the system. It was worth noting that the existing form of 4 % and 8 % water had not changed, while the signal peak of 12 % free water was close to 0. This is attributed to the reduced water retention capacity of the system due to the increase in butter component (Wang, et al., 2022). Further, the content of polysaccharides hydrophilic groups in the system turns lower and the excessive hydrophobic groups in butter are exposed. Subsequently, the evaporation of free water is promoted by thermodynamics in the system (Kong, et al., 2023). However, the percentage of free water in the steaming sample increased. The primary reason is that heating accelerated the gelatinization of the gel (He, et al., 2021). In other words, because the water on the surface of the ink evaporated rapidly and disappeared, and then the outer structure tended to stabilize, thus reducing the speed of internal water transfer and diffusion (Thongcharoenpipat and Yamsaengsung, 2023). More importantly, the peak time of the three signal peaks in the steaming sample occurred earlier than that in the untreated group, indicating that the steaming treatment promoted the stability of moisture in the gel.

4. Conclusion

In this study, *P. ostreatus* was successfully extruded as the main ink for 3DP, and the printing system of POP-40 % exhibited a constructive appearance and self-supporting ability. The stable molecular structure and water holding capacity in POP-40 % system prompted its dense internal structure, because of the bond energy interaction between proteins and polysaccharides in the *P. ostreatus*, and water. Afterwards, the addition of butter improved the brightness of the *P. ostreatus* system but led to poor orderliness of the internal structure. This may be attributed to the formation of carbohydrate-lipid complexes, resulting in the structure and stability changes of the system. Further experiments are required to validate this observation. Although, the steaming successfully conquered the reduction of the stability of the system with a superb accuracy for Steaming-5min. Steaming enhanced the water holding capacity of the system by promoting the stability of intermolecular hydrogen bonds, thereby improving printing accuracy. Therefore, the study demonstrated the significant potential of *P. ostreatus* ink for 3DP, offering insights for the development of edible fungi 3DP products and the precise manufacturing of 3D-printed items.

CRediT authorship contribution statement

Rui Liu: Conceptualization, Data curation, Investigation, Formal analysis, Writing – original draft. **Qiuhui Hu:** Conceptualization, Methodology, Funding acquisition, Project administration. **Gaoxing Ma:** Writing – review & editing, Methodology, Supervision. **Fei Pei:** Writing – review & editing, Formal analysis. **Liyan Zhao:** Writing –

review & editing, Supervision. **Ning Ma:** Writing – review & editing, Formal analysis. **Fan Yang:** Writing – review & editing. **Xiao Liu:** Writing – review & editing. **Anxiang Su:** Conceptualization, Methodology, Formal analysis, Writing – original draft, Writing – review & editing.

Declaration of competing interest

The authors declare that they have no known competing financial interests or personal relationships that could have appeared to influence the work reported in this paper.

Data availability

Data will be made available on request.

Acknowledgements

This study was financial supported by The Key Research and Development Program of Jiangsu Province (BE2022378) and Jiangsu Province Agricultural Science and Technology Innovation Fund (CX (21) 2005).

References

Abdel-Aal, E.-S.M., Hernandez, M., Rabalski, I., Hucl, P., 2020. Composition of hairless canary seed oil and starch-associated lipids and the relationship between starch pasting and thermal properties and its lipids. LWT (Lebensm.-Wiss. & Technol.) 125, 109257. https://doi.org/10.1016/j.lwt.2020.109257.

Adedeji, O.E., Choi, J.-Y., Park, G.E., Kang, H.J., Aminu, M.O., Min, J.H., Chinma, C.E., Moon, K.-D., Jung, Y.H., 2022. Formulation and characterization of an interpenetrating network hydrogel of locust bean gum and cellulose microfibrils for 3D printing. Innov Food Sci. Emerg. Technol. 80, 103086 https://doi.org/10.1016/j.ifset.2022.103086.

Anukiruthika, T., Moses, J.A., Anandharamakrishnan, C., 2020. 3D printing of egg yolk and white with rice flour blends. J. Food Eng. 265, 109291 https://doi.org/10.1016/j.jfoodeng.2019.109691.

Baiano, A., 2022. 3D printed foods: a comprehensive review on technologies, nutritional value, safety, consumer attitude, regulatory framework, and economic and sustainability issues. Food Rev. Int. 38 (5), 986–1016. https://doi.org/10.1080/87559129.2020.1762091.

Barragan-Martinez, L.P., Roman-Guerrero, A., Vernon-Carter, E.J., Alvarez-Ramirez, J., 2022. Impact of fat replacement by a hybrid gel (canola oil/candelilla wax oleogel and gelatinized corn starch hydrogel) on dough viscoelasticity, color, texture, structure, and starch digestibility of sugar-snap cookies. Int. J. Gastron. Food Sci. 29, 100563 https://doi.org/10.1016/j.ijgfs.2022.100563.

Chen, J., Cai, H., Zhang, M., Chen, Z., 2023. Effects of rice protein on the formation and structural properties of starch-lipid complexes in instant rice noodles incorporated with different fatty acids. Food Biosci. 54, 102851 https://doi.org/10.1016/j.fbio.2023.102851.

Du, J., Zhou, C., Xia, Q., Wang, Y., Geng, F., He, J., Sun, Y., Pan, D., Cao, J., 2022. The effect of fibrin on rheological behavior, gelling properties and microstructure of myofibrillar proteins. LWT (Lebensm.-Wiss. & Technol.) 153, 112457. https://doi.org/10.1016/j.lwt.2021.112457.

Fernandes, A.S., Neves, B.V., Mazzo, T.M., Longo, E., Jacob-Lopez, E., Zepka, L.Q., de Rosso, V.V., 2023. Bigels as potential inks for extrusion-based 3d food printing: effect of oleogel fraction on physical characterization and printability. Food Hydrocolloids 144, 108986. https://doi.org/10.1016/j.foodhyd.2023.108986.

Fan, F., Li, S., Huang, W., Ding, J., 2022. Structural characterization and fluidness analysis of lactose/whey protein isolate composite hydrocolloids as printing materials for *3D* printing. Food Res. Int. 152, 110908 https://doi.org/10.1016/j.foodres.2021.110908.

Guénard-Lampron, V., Masson, M., Leichtnam, O., Blumenthal, D., 2021. Impact of 3D printing and post-processing parameters on shape, texture and microstructure of carrot appetizer cake. Innov. Food Sci. Emerg. Technol. 72, 102738 https://doi.org/10.1016/j.ifset.2021.102738.

Guo, C., Zhang, M., Bhandari, B., 2019. Model building and slicing in food 3D printing processes: a review. Compr. Rev. Food Sci. Food Saf. 18 (4), 1052–1069. https://doi.org/10.1111/1541-4337.12443.

Guo, C., Zhang, M., Devahastin, S., 2021. Color/aroma changes of 3D-Printed buckwheat dough with yellow flesh peach as triggered by microwave heating of gelatin-gum Arabic complex coacervates. Food Hydrocolloids 112, 106358. https://doi.org/10.1016/j.foodhyd.2020.106358.

Guerrero, P., Beatty, E., Kerry, J., Caba, K., 2012. Extrusion of soy protein with gelatin and sugars at low moisture content. J. Food Eng. 110 (1), 53–59. https://doi.org/10.1016/j.jfoodeng.2011.12.009.

Hamza, A., Ghanekar, S., Santhosh Kumar, D., 2023. Current trends in health-promoting potential and biomaterial applications of edible mushrooms for human wellness. Food Biosci. 51, 102290 https://doi.org/10.1016/j.fbio.2022.102290.

He, A., Xu, J., Hu, Q., Zhao, L., Ma, G., Zhong, L., Liu, R., 2023. Effects of gums on 3D printing performance of *Pleurotus eryngii* powder. J. Food Eng. 351, 111514 https://doi.org/10.1016/j.jfoodeng.2023.111514.

He, C., Zhang, M., Devahastin, S., 2021. Microwave-induced deformation behaviors of 4D printed starch-based food products as affected by edible salt and butter content. Innov. Food Sci. Emerg. Technol. 70, 102699 https://doi.org/10.1016/j.ifset.2021.102699.

Hsieh, C., Chang, C., Wong, L., Hu, C., Lin, J., Hsieh, C., 2020. Alternating current electric field inhibits browning of *Pleurotus ostreatus via* inactivation of oxidative enzymes during postharvest storage. LWT (Lebensm.-Wiss. & Technol.) 134, 110212. https://doi.org/10.1016/j.lwt.2020.110212.

Ji, S.Y., Xu, T., Liu, Y., Li, H.Y., Luo, J.Y., Zou, Y.C., Zhong, Y.H., Li, Y., Lu, B.Y., 2022. Investigation of the mechanism of casein protein to enhance 3D printing accuracy of cassava starch gel. Carbohydr. Polym. 295, 119827 https://doi.org/10.1016/j.carbpol.2022.119827.

Ji, Y., Hu, Q., Ma, G., Yu, A., Zhao, L., Zhang, X., Zhao, R., 2022. Selenium biofortification in *Pleurotus eryngii* and its effect on lead adsorption of gut microbiota via in *vitro* fermentation. Food Chem. 396 (1), 133664 https://doi.org/10.1016/j.foodchem.2022.133664.

Jiang, H., Zheng, L., Zou, Y., Tong, Z., Han, S., Wang, S., 2019. 3D food printing: main components selection by considering rheological properties. Crit. Rev. Food Sci. Nutr. 59 (14), 2335–2347. https://doi.org/10.1080/10408398.2018.1514363.

Jiang, Q., Zhang, M., Mujumdar, A.S., 2022. Novel evaluation technology for the demand characteristics of 3D food printing materials: a review. Crit. Rev. Food Sci. Nutr. 62 (17), 4669–4683. https://doi.org/10.1080/10408398.2021.1878099.

Kong, D., Zhang, M., Mujumdar, A.S., Li, J., 2023. Feasibility of hydrocolloid addition for 3D printing of Qingtuan with red bean filling as a dysphagia food. Food Res. Int. 165, 112469 https://doi.org/10.1016/j.foodres.2023.112469.

Lin, Q., Shang, M., Li, X., Sang, S., Chen, L., Long, J., Jiao, A., Ji, H., Qiu, C., Jin, Z., 2024. Rheology and 3D printing characteristics of heat-inducible pea protein-carrageenan-glycyrrhizic acid emulsions as edible inks. Food Hydrocolloids 147, 109347. https://doi.org/10.1016/j.foodhyd.2023.109347.

Liu, L., Hu, X.Z., Zou, L., 2023. Wheat polysaccharides and gluten effect on water migration and structure in noodle doughs: an ^{1}H LF-NMR study. J. Cereal. Sci. 110, 103628 https://doi.org/10.1016/j.jcs.2023.103628.

Liu, Y., Zhang, H., Brennan, M., Brennan, C., Qin, Y., Cheng, G., Liu, Y., 2022. Physical, chemical, sensorial properties and in vitro digestibility of wheat bread enriched with yunnan commercial and wild edible mushrooms. LWT (Lebensm.-Wiss. & Technol.) 169, 113923. https://doi.org/10.1016/j.lwt.2022.113923.

Liu, Z., Xing, X., Xu, D., Chitrakar, B., Hu, L., Hati, S., Mo, H., Li, H., 2022. Correlating rheology with 3D printing performance based on thermo-responsive κ-carrageenan/*Pleurotus ostreatus* protein with regard to interaction mechanism. Food Hydrocolloids 131, 107813. https://doi.org/10.1016/j.foodhyd.2022.107813.

Lv, Y., Lv, W., Li, G., Zhong, Y., 2023. The research progress of physical regulation techniques in 3D food printing. Trends Food Sci. Technol. 133, 231–243. https://doi.org/10.1016/j.tifs.2023.02.004.

Lv, S., Li, H., Liu, Z., Cao, S., Yao, L., Zhu, Z., Hu, L., Xu, D., Mo, H., 2024. Preparation of *Pleurotus eryngii* protein baked food by 3D printing. J. Food Eng. 365, 11845 https://doi.org/10.1016/j.jfoodeng.2023.111845.

Ma, J., Liu, X., Wang, K., Jin, Y., Liu, Y., 2024. New insight into yolk sphere microgel structure impacted by lipid and protein distribution changing under heating processing. Food Chem. 435, 137520 https://doi.org/10.1016/j.foodchem.2023.137520.

Méndez-Cid, F.J., Centeno, J.A., Martínez, S., Carballo, J., 2017. Changes in the chemical and physical characteristics of cow's milk butter during storage: effects of temperature and addition of salt. J. Food Compos. Anal. 63, 121–132. https://doi.org/10.1016/j.jfca.2017.07.032.

Nie, Y., Liu, Y., Jiang, J., Xiong, Y.L., Zhao, X., 2022. Rheological, structural, and water-immobilizing properties of mung bean protein-based fermentation-induced gels: effect of pH-shifting and oil imbedment. Food Hydrocolloids 129, 107607. https://doi.org/10.1016/j.foodhyd.2022.107607.

Nooshkam, M., Varidi, M., Bashash, M., 2019. The Maillard reaction products as food-born antioxidant and antibrowning agents in model and real food systems. Food Chem. 275, 644–660. https://doi.org/10.1016/j.foodchem.2018.09.083.

Qiu, C., Wang, C., Li, X., Sang, S., McClements, D.J., Chen, L., Long, J., Jiao, A., Wang, J., Jin, Z., 2023. Preparation of high internal phase Pickering emulsion gels stabilized by glycyrrhizic acid-zein composite nanoparticles: gelation mechanism and 3D printing performance. Food Hydrocolloids 135, 108128. https://doi.org/10.1016/j.foodhyd.2022.108128.

Shi, Y., Zhang, M., Phuhongsung, P., 2022. Microwave-induced spontaneous deformation of purple potato puree and oleogel in 4D printing. J. Food Eng. 313, 110757 https://doi.org/10.1016/j.jfoodeng.2021.110757.

Sołowiej, B.G., Nastaj, M., Waraczewski, R., Szafrańska, J.O., Muszyński, S., Radzki, W., Mleko, S., 2023. Effect of polysaccharide fraction from oyster mushroom (*Pleurotus ostreatus*) on physicochemical and antioxidative properties of acid casein model processed cheese. Int. Dairy J. 137, 105516 https://doi.org/10.1016/j.idairyj.2022.105516.

Thongcharoenpipat, C., Yamsaengsung, R., 2023. Microwave-assisted vacuum frying of durian chips: impact of ripening level on the drying rate, physio-chemical characteristics, and acceptability. Food Bioprod. Process. 138, 40–52. https://doi.org/10.1016/j.fbp.2023.01.001.

Wang, H., Li, X., Wang, J., Vidyarthi, S.K., Wang, H., Zhang, X., Gao, L., Yang, K., Zhang, J., Xiao, H., 2022. Effects of postharvest ripening on water status and

distribution, drying characteristics, volatile profiles, phytochemical contents, antioxidant capacity and microstructure of kiwifruit (*Actinidia deliciosa*). Food Control 139, 109062. https://doi.org/10.1016/j.foodcont.2022.109062.

Wang, L., Brennan, M.A., Guan, W., Liu, J., Zhao, H., Brennan, C.S., 2021. Edible mushrooms dietary fibre and antioxidants: effects on glycaemic load manipulation and their correlations pre-and post-simulated *in vitro* digestion. Food Chem. 351, 129320 https://doi.org/10.1016/j.foodchem.2021.129320.

Wang, Y., Yang, F., Wu, M., Li, J., Bai, Y., Xu, W., Qiu, S., 2020. Synergistic effect of pH shifting and mild heating in improving heat induced gel properties of peanut protein isolate. LWT (Lebensm.-Wiss. & Technol.) 131, 109812. https://doi.org/10.1016/j.lwt.2020.109812.

Wedamulla, N.E., Fan, M.Q., Choi, Y.J., Kim, E.K., 2023. Effect of pectin on printability and textural properties of potato starch 3D food printing gel during cold storage. Food Hydrocolloids 137, 108362. https://doi.org/10.1016/j.foodhyd.2022.108362.

Wen, Y., Che, Q., Kim, H., Park, H., 2021. Potato starch altered the rheological, printing, and melting properties of 3D-printable fat analogs based on inulin emulsion-filled gels. Carbohydr. Polym. 269, 118285 https://doi.org/10.1016/j.carbpol.2021.118285.

Wen, Y., Kim, H., Park, H., 2022. Effect of xylose on rheological, printing, color, texture, and microstructure characteristics of 3D-printable colorant-containing meat analogs based on mung bean protein. Food Res. Int. 160, 111704 https://doi.org/10.1016/j.foodres.2022.111704.

Xu, F., Liu, W., Zhang, L., Liu, Q., Wang, F., Zhang, H., Hu, H., Blecker, C., 2022. Thermal, structural, rheological and morphological properties of potato starch-gluten model dough systems: effect of degree of starch pre-gelatinization. Food Chem. 396, 133628 https://doi.org/10.1016/j.foodchem.2022.133628.

Xu, J., Xu, D., Hu, Q., Ma, N., Pei, F., Su, A., Ma, G., 2022. Immune regulatory functions of biologically active proteins from edible fungi. Front. Immunol. 13, 1034545 https://doi.org/10.3389/fimmu.2022.1034545.

Yu, J., Wang, X., Li, D., Wang, L., Wang, Y., 2022. Development of soy protein isolate emulsion gels as extrusion-based 3D food printing inks: effect of polysaccharides incorporation. Food Hydrocolloids 131, 107824. https://doi.org/10.1016/j.foodhyd.2022.107824.

Zhang, L., Zhou, C., Xing, S., Chen, Y., Su, W., Wang, H., Tan, M., 2023. Sea bass protein-polyphenol complex stabilized high internal phase of algal oil Pickering emulsions to stabilize astaxanthin for 3D food printing. Food Chem. 417, 135824 https://doi.org/10.1016/j.foodchem.2023.135824.

Zhao, X., Guo, R., Li, X., Wang, X., Zeng, L., Wen, X., Huang, Q., 2023. Effect of oil-modified crosslinked starch as a new fat replacer on gel properties, water distribution, and microstructures of pork meat batter. Food Chem. 409, 135337 https://doi.org/10.1016/j.foodchem.2022.135337.

Zheng, C., Li, J., Liu, H., Wang, Y., 2023. Review of postharvest processing of edible wild-grown mushrooms. Food Res. Int. 173, 113223 https://doi.org/10.1016/j.foodres.2023.113223.

Zheng, M., Xiao, Y., Yang, S., Liu, H., Liu, M., Yaqoob, S., Xu, X., Liu, J., 2020. Effects of heat-moisture, autoclaving, and microwave treatments on physicochemical properties of proso millet starch. Food Sci. Nutr. 8 (2), 735–743. https://doi.org/10.1002/fsn3.1295.